


Understanding hand-object manipulation by modeling the contextual relationship between actions, grasp types and object attributes

Journal Title
XX(X):1-14
©The Author(s) 2016
Reprints and permission:
sagepub.co.uk/journalsPermissions.nav
DOI: 10.1177/ToBeAssigned
www.sagepub.com/


Minjie Cai¹, Kris M. Kitani² and Yoichi Sato¹

Abstract

This paper proposes a novel method for understanding daily hand-object manipulation by developing computer vision-based techniques. Specifically, we focus on recognizing hand grasp types, object attributes and manipulation actions within a unified framework by exploring their contextual relationships. Our hypothesis is that it is necessary to jointly model hands, objects and actions in order to accurately recognize multiple tasks that are correlated to each other in hand-object manipulation. In the proposed model, we explore various semantic relationships between actions, grasp types and object attributes, and show how the context can be used to boost the recognition of each component. We also explore the spatial relationship between the hand and object in order to detect the manipulated object from hand in cluttered environment. Experiment results on all three recognition tasks show that our proposed method outperforms traditional appearance-based methods which are not designed to take into account contextual relationships involved in hand-object manipulation. The visualization and generalizability study of the learned context further supports our hypothesis.

Keywords

Manipulation action, grasp type, object attribute, contextual relationship

1 Introduction

The understanding of hand-object manipulation (HOM) is concerned with how the hand interacts with the object under certain purpose, requiring information such as the poses of a hand for holding/manipulating an object, the attribute information of the manipulated object and the undergoing action. The ability to understand HOM activities automatically from visual sensing is important for the robotics community with potential applications such as robotic hand design and robotic action learning. In robotic hand design, the study of hand grasping behavior in daily manipulation tasks provides critical information about hand functions that can be used for robotic hand development (Cutkosky (1989); Zheng et al. (2011); Bullock et al. (2013a); Dollar (2014)). It can also facilitate robotic action learning by studying the relationship between different components (hands, objects and actions) in performing a manipulation task (Feix et al. (2014a); Yang et al. (2015b)).

In this work, we aim to recognize grasp types, object attributes and actions of manipulation tasks recorded with a wearable camera. The three terms provide very useful information for understanding HOM activities, and are defined as follows: *Grasp types* are a discrete set of canonical hand poses often used to describe various strategies for holding objects stably in hand. For example, the use of all fingers around a curved object like a cup is called a medium wrap. *Object attributes* characterize physical properties of the objects such as rigidity and shape. *Actions* in this work refer to different patterns of hand-object interactions such as open or pour. A wearable camera

enables continuous recording of unconstrained hand-object interactions and offers an ideal viewing perspective for recording and studying manipulation activities in real-life settings. However, the recognition of real-world HOM activities is challenging. There are often occlusions of a hand, especially fingers, during hand-object interactions, making it hard to observe and recognize hand grasps. It is also challenging to detect the manipulated object and infer its attribute information in cluttered background. Although recent years have seen the popularity of deep learning techniques in various vision recognition tasks, their performance is often limited with insufficient training data and the correlation between different recognition tasks of hands, objects and actions are not considered.

In this work, we propose a unified model (Figure 1) in which the grasp types, object attributes and actions are recognized together by exploring their contextual relationships. Our hypothesis is that the actions, hands and objects are strongly correlated with each other in HOM activities, and thereby it is important to jointly model them together. Jointly modeling hand grasps, objects and actions has its empirical basis in neuroscience and psychology (Kjellstrom et al. (2008); Feix et al. (2014b)),

¹Institute of Industrial Science, The University of Tokyo, Japan

²Robotics Institute, Carnegie Mellon University, USA

Corresponding author:

Minjie Cai, Institute of Industrial Science, The University of Tokyo, Komaba 4-6-1, Meguro-ku, Tokyo 153-8505, Japan.

Email: cai-mj@iis.u-tokyo.ac.jp

arXiv:1807.08254v1 [cs.CV] 22 Jul 2018

and our work firstly presents a computational way to explicitly modeling these relationships. Specifically, three kinds of contextual relationships are studied in the proposed model. The *functional context* models the functional constraints on grasp types and object attributes within different manipulation actions. The *physical context* models the semantic relationship between hand grasp types and attributes of the grasped object under physical constraints. The *spatial context* models the spatial relationship between the hand and the manipulated object. With these contextual relationships serving as high-level constraints, we utilize deep Convolutional Neural Networks (CNNs) to model the visual evidence for grasp types, object attributes and actions respectively. In particular, we develop a CNN to detect the hand and the grasped object simultaneously based on spatial hand-object relationship. We show in experiments that our method significantly improves the recognition performance of all three tasks compared with previous approaches which did not consider mutual context involved in these tasks. Generalizability study further indicates that the contextual relationships are consistent across different datasets and therefore could be exploited as common knowledge in understanding hand-object manipulation.

Overall, this paper extends our previous work that was published in [Cai et al. \(2016\)](#). Novel contributions over our previous publication are summarized as follows:

- An unified model is constructed for studying various contextual relationships between hands, objects and actions together (Section 3).
- A detection CNN is developed to detect hand and object simultaneously (Section 4.2).
- An iterative inference method is developed to optimize multiple tasks together (Section 5).
- More detailed visualization and analysis of the experiment results is provided (Section 6).

The rest of the paper is organized as follows. Section 2 presents related work. The architecture and each component of our proposed model are described in Section 3. Section 4 and Section 5 elaborate the details of learning and inference of the model. Experiment results are given in Section 6. Section 7 concludes the paper and discusses future work.

2 Related Work

Hand grasp has been studied for decades to better understand the use of human hands ([Napier \(1956\)](#); [Santello et al. \(1998\)](#); [Romero et al. \(2013\)](#); [Bullock et al. \(2013b\)](#); [Huang et al. \(2015\)](#)). Grasp taxonomies have also been proposed to facilitate hand grasp analysis ([Cutkosky \(1989\)](#); [Kang and Ikeuchi \(1993\)](#); [Feix et al. \(2009\)](#); [Liu et al. \(2014\)](#); [Feix et al. \(2016\)](#)). Approaches for vision-based hand grasp analysis were developed primarily in structured environment where hand-object interactions are well recorded by camera arrays or depth sensors ([Kjellstrom et al. \(2008\)](#); [Hamer et al. \(2009\)](#); [Oikonomidis et al. \(2011\)](#); [Romero et al. \(2013\)](#)). [Cai et al. \(2015\)](#) first developed appearance-based method to recognize hand grasp types from manipulation tasks recorded in real-world environment with a wearable RGB camera. [Saran et al. \(2015\)](#) then used detected hand parts as intermediate representation to distinguish between

fine-grained grasp types. [Yang et al. \(2015a\)](#) and [Rogez et al. \(2015\)](#) further utilized deep learning techniques to improve grasp recognition performance. Nevertheless, hand grasp recognition on 2D images still remains a challenging problem due to limited view of hand appearance and visual ambiguity between different grasp types ([Cai et al. \(2017\)](#)).

Visual attributes (physical properties inferred from image appearance) are often used as intermediate representation for many applications, such as object recognition ([Farhadi et al. \(2009\)](#); [Lampert et al. \(2009\)](#); [Vedaldi et al. \(2014\)](#)), facial verification ([Kumar et al. \(2009\)](#)), image retrieval and tagging ([Siddiquie et al. \(2011\)](#); [Parikh and Grauman \(2011\)](#); [Zhang et al. \(2014\)](#)). [Lampert et al. \(2009\)](#) performs object detection based on a human-specified high-level description of the target classes for which no training examples are available. The description consists of attributes like shape, color or even geographic information. [Parikh and Grauman \(2011\)](#) explored the relative strength of attributes by learning a rank function for each attribute which can be used to generate richer textual descriptions. In this work, we extract attribute information from the manipulated object and use it as context to improve the recognition performance of grasp types and actions.

The correlations between objects and hand grasps in hand-object interactions have been widely studied in neuroscience and psychology. It has been shown that humans use the same or similar grasp types for certain types of objects, and the shape of the object has a large influence on the applied grasp ([Klatzky et al. \(1987\)](#); [Gilster et al. \(2012\)](#)). Recently, [Feix et al. \(2014a\)](#) investigated the relationship between grasp types and object attributes in a large real-world human grasping dataset by manual inspection. In our prior work ([Cai et al. \(2016\)](#)), a Bayesian network is trained to automatically learn the contextual relationship between grasp types and object attributes. The context information has then been used to improve the recognition performance of both grasp types and object attributes. In this paper, we extend our prior work to incorporate the context from actions in a more complete model.

Recognizing actions of hand-object interactions under first-person vision paradigm has become attractive in recent years since a wearable camera provides an ideal viewing perspective for recording and analyzing hand-object interactions. [Fathi et al. \(2011, 2012\)](#) used appearance around the regions of hand-object interactions to recognize egocentric actions. [Pirsiavash and Ramanan \(2012\)](#) has shown that detecting objects in the scene helps to infer daily hand activities. [Li et al. \(2015\)](#) performed a systematic evaluation of different features and provided a list of best practices of combining different cues for activity recognition. [Ma et al. \(2016\)](#) further proposed a deep learning architecture for egocentric action recognition, which integrates both appearance and motion information. However, previous work only treated hand activity recognition as an image or video classification problem without full understanding of the semantic relationships involved. We argue that it is important to obtain a detailed understanding of the interactions between the hands and the objects in HOM activities. Our work is inspired by a number of works that studied the interactions between human poses and objects

in human activities (Singh et al. (2010); Yao and Fei-Fei (2010); Sadeghi and Farhadi (2011)). Different from these work, we aim to better understand HOM activities by modeling the contextual relationships between actions, hand grasp types and object attributes.

3 Architecture

Our goal is to recognize the hand grasp type, attribute information of the manipulated object, and the manipulation action within a HOM activity. Based on our hypothesis that hands, objects and actions are correlated with each other in HOM activities, we propose a novel model to jointly infer grasp types, object attributes and actions by exploring their contextual relationships in an unified framework.

Figure 1 illustrates the proposed model. The model can be considered as a conditional random field. Given an image (or image sequence) I of HOM activities, we jointly model the action class A , the hands $H = \{H^l, H^r\}$ with grasp types $G = \{G^l, G^r\}$, and the attributes of the manipulated objects $O = \{O^l, O^r\}$. l, r indicate the left and right side respectively. The proposed model could be understood functionally as two different parts: The first part models different contextual relationships between hands, objects and actions. The second part models visual evidence of grasp types, object attributes, and actions conditioned on image appearance. Overall, the model is represented as

$$\Psi(A, G, O, H|I) = \Psi_{FC}(A, G, O) + \Psi_{PC}(G, O) + \Psi_{SC}(H, O) + \Psi_G(G, H|I) + \Psi_O(O|I) + \Psi_A(A|I), \quad (1)$$

where Ψ_{FC} models the semantic relationship between actions, grasp types and object attributes under functional constraints, Ψ_{PC} models the semantic relationship between grasp types and object attributes under physical constraints, Ψ_{SC} models the spatial relationship between the hand and the grasped object, Ψ_G, Ψ_O, Ψ_A models the visual evidence based on discriminative classifiers trained for grasp types, object attributes and actions respectively. Next, we explain the details of each component.

3.1 Functional context

We first consider the functional context denoted as $\Psi_{FC}(A, G, O)$ which models the contextual relationship between actions, grasp types and object attributes under functional constraints. It is observed that grasp types together with object attributes provide complementary characterization for the functionality of different manipulation actions. For example, given a pen, the grasp type of *writing tripod* reveals the functionality of action *write*, while the grasp type of *thumb-2 finger* reveals the functionality of action *take*. On the other hand, the knowledge of the action being performed provides functional constraints on the hand grasp type and the attributes of the manipulated object. For example, the action of *scoop* indicates the high probability of combination of a container (such as a bottle) held by some power grasp and a long-shape tool (such as a spoon) held by some precision grasp. Therefore, $\Psi_{FC}(A, G, O)$ is parameterized

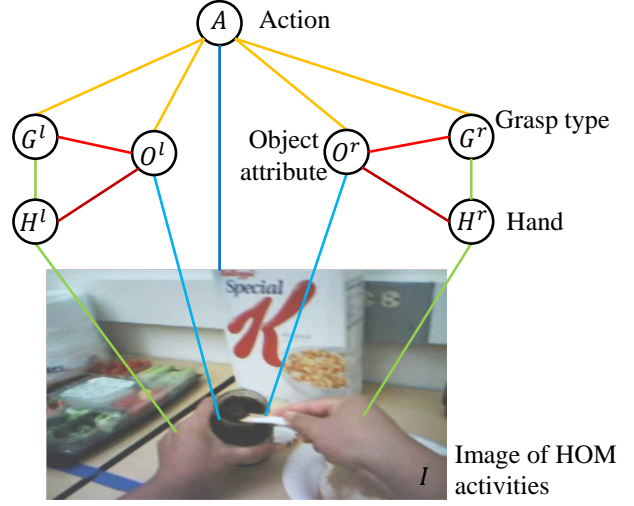


Figure 1. An illustration of our proposed graphical model. A denotes the hand action class, G the grasp type class, O the object attribute class, and P the spatial positions of hands and objects. We define G and O for both two hands. The edges denoted by different colors correspond to different components of our model.

as

$$\Psi_{FC}(A, G, O) = \sum_{k=1}^{N_a} \sum_{i,j=0}^{N_g} \sum_{m,n=0}^{N_o} \mathbf{1}_{(A=a_k)} \cdot \mathbf{1}_{(G^l=g_i)} \cdot \mathbf{1}_{(G^r=g_j)} \cdot \mathbf{1}_{(O^l=o_m)} \cdot \mathbf{1}_{(O^r=o_n)} \cdot \alpha_{k,i,j,m,n}, \quad (2)$$

where N_a is the number of action classes and a_k denotes the k -th action class. N_g is the number of grasp types and g_i/g_j denotes the i/j -th grasp type ($i/j = 0$ means no hand). N_o is the number of object attributes and o_m/o_n denotes the m/n -th object attribute ($m/n = 0$ means no object). $\mathbf{1}_{(\cdot)}$ is an indicator function and has value 1 when the condition inside (\cdot) is fulfilled, otherwise 0. $\alpha_{k,i,j,m,n}$ indicates the strength of functional compatibility between the action a_k , the grasp type g_i, g_j and object attribute o_m, o_n at the left hand and the right hand (l, r indicate the side).

3.2 Physical context

We also model the contextual relationship between grasp types and object attributes under physical constraints as denoted by $\Psi_{PC}(G, O)$. Object attributes pose physical constraints on the affordance of different grasp types. For example, a bottle cap with a round shape is more likely to be held with the grasp type of *precision sphere* than with other grasp types. Hence, with the knowledge of object attributes, we obtain a prior information about the possibility of different grasp types. On the other hand, knowing the grasp type also reveals attributes of the grasped object. Therefore, $\Psi_{PC}(G, O)$ is parameterized as

$$\Psi_{PC}(G, O) = \sum_{s \in \{l,r\}} \sum_{i=1}^{N_g} \sum_{m=1}^{N_o} \mathbf{1}_{(G^s=g_i)} \cdot \mathbf{1}_{(O^s=o_m)} \cdot \beta_{i,m}, \quad (3)$$

where s indicates the side of hand. N_g, N_o, g_i, o_m have the same meaning as described in Section 3.1. $\beta_{i,m}$ indicates the

strength of physical constraints between grasp type g_i and object attribute o_m .

3.3 Spatial context

In addition to the above semantic relationships, we also explore the spatial context between the hand and grasped object denoted as $\Psi_S C(H, O)$. Unlike the hand that has unique skin color and consistent size, object has inconsistent appearance and is often partially occluded by the hand during manipulation. Hence, the task of object detection is more challenging than hand detection. In this work we propose to explore the spatial context of hand for estimating the location of the grasped object. We observe that hand appearance provides important hint about the relative location and size of the grasped part of the object (not the whole object, and we will refer to ‘‘grasped part of the object’’ simply as ‘‘object’’ in the rest of paper). For instance, object size is related to hand opening and relative object location is consistent with hand orientation. The spatial context of $\Psi_S C(H, O)$ is represented as

$$\Psi_{SC}(H, O) = \sum_{s \in \{l, r\}} \gamma_s \cdot p(P_o^s | P_{h \rightarrow o}^s), \quad (4)$$

where $p(P_o^s | P_{h \rightarrow o}^s)$ is the likelihood of observing P_o^s , the object location, given the reference object location $P_{h \rightarrow o}^l$ estimated from the s -side hand region, and is computed by intersection over union of the two object locations (bounding boxes). γ_s is the weight for the spatial relationship between the hand and the grasped object.

3.4 Grasp types

$\Psi_G(G, H, I)$ models visual evidence of grasp types. It is further composed by two components. The first component models the likelihood of detecting the hand H in image I . The second components models the visual belief of the grasp type G conditioned on image appearance within H . $\Psi_G(G, H, I)$ is represented as

$$\Psi_G(G, H|I) = \sum_{s \in \{l, r\}} \left(\zeta_s^T \cdot \phi_h(P_h^s | I) + \sum_{i=1}^{N_g} \mathbf{1}_{(G^s = g_i)} \cdot \eta_i^T \cdot \phi_g(P_h^s) \right), \quad (5)$$

where $\phi_h(P_h^s | I)$ is the vector of hand detection scores obtained from a hand detector, and $\phi_g(P_h^s)$ is the vector of classification scores obtained from a grasp type classifier. ζ_s is the set of weights for the detection scores corresponding to the s -side hand, and η_i is the set of weights for the classification scores corresponding to grasp type g_i .

3.5 Object attributes

Similar to grasp types, $\Psi_O(O, I)$ models visual evidence for object attributes. However, the object location is not directly modeled from image appearance (it is modeled by spatial context in Section 3.3). $\Psi_O(O, I)$ is represented as

$$\Psi_O(O|I) = \sum_{s \in \{l, r\}} \sum_{m=1}^{N_o} \mathbf{1}_{(O^s = o_m)} \cdot \lambda_m^T \cdot \phi_o(P_o^s), \quad (6)$$

where $\phi_o(P_o^s)$ is the output of object attribute classifier obtained from the object region in P_o^s . λ_m encodes the set of weights for the classification scores corresponding to object attribute o_m .

3.6 Actions

$\Psi_A(A, I)$ models visual evidence for manipulation actions. Different from grasp types and object attributes which are recognized from image regions after a detection procedure, actions are recognized directly from a whole image. $\Psi_A(A, I)$ is represented as

$$\Psi_A(A|I) = \sum_{i=1}^{N_a} \mathbf{1}_{(A = a_i)} \cdot \xi_i^T \cdot \phi_a(I), \quad (7)$$

where $\phi_a(I)$ is the output vector of an action classifier. ξ_i is the set of weights corresponding to action class a_i .

4 Learning

In this section, we describe the approaches for learning different components of our model. We first introduce the class definition of grasp types and object attributes in Section 4.1 that are important components of the model. We then show how to train hand and object detector in Section 4.2, and train classifiers for grasp types, object attributes and actions in Section 4.3. We explain how to learn the model parameters in Section 4.4. Implementation details about the utilized CNNs are given in Section 4.5.

4.1 Class definition

4.1.1 Grasp types Hand grasp types are important for understanding HOM activities since they characterize how hands hold the objects, as well as the action functionality to be implemented. A number of work (Cutkosky (1989); Feix et al. (2016)) have investigated the categorization of hand poses when holding an object into a discrete set of types to facilitate the study of hand grasps. The resulting grasp taxonomies are created according to some classification criterion mainly based on functionality, object shape, and finger articulation. A commonly used grasp taxonomy is illustrated in Figure 2. However, it is not an appropriate way to use the full sized taxonomy for any specific tasks as the proportion of different grasp types varies a lot. It also has been shown in Cai et al. (2017) that there is a trade-off between the size of grasp taxonomy and the classification accuracy. In this work, we adopt an unsupervised clustering method of Huang et al. (2015) to first discover a diverse set of hand grasps based on hand appearance from the dataset being used. Then the obtained clusters of hand images are examined with existing grasp taxonomy to define the set of grasp types to be used in the current task. We assign new grasp type to those clusters whose hand poses are undefined in existing grasp taxonomies, and discard the clusters with small member size. The details of the used grasp types are described later in experiments.

4.1.2 Object attributes Attributes of the manipulated object are also important for understanding HOM activities since they reflect possible grasp types and actions that are affordable. Given an object with long and thin shape (like a



Figure 2. Examples of hand grasp types from a commonly used grasp taxonomy defined in Feix et al. (2009). Images are adapted from Cai et al. (2015).



Figure 3. Example images of four different attributes: *prismatic*, *round*, *flat*, and *deformable*.

pen), the hand is more likely to perform the action of *writing* instead of *drinking*. While objects can be assessed by a wide range of attributes (shape, weight, surface smoothness, etc.), we only focus on attributes that are relevant to grasping and are also possible to be learned from image appearance. Figure 3 shows some examples of the attributes studied in this work, three of which are related to object shape and the fourth is related to object rigidity. We identify three different shapes based on the criterion in Table 1. The fourth attribute of *deformable* identifies the object that deforms under normal grasping forces. Examples are a sponge or a rag. In this work, we aim to characterize and classify the manipulated object based on the composition of these attributes.

Table 1. Classification criterion of three shape classes. Length of object along three object dimensions (major axes of the object) are denoted as A , B , and C , where $A \geq B \geq C$.

Shape classes	Object dimensions
Prismatic	$A > 2B$
Round	$B \leq A < 2B, C \leq A < 2C$
Flat	$B > 2C$

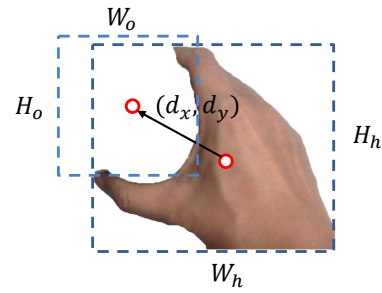


Figure 4. Illustration of relative location and scale of the hand and the grasped object.

4.2 Training detectors

Object detection is a challenging task in computer vision, particularly unreliable when there are occlusions during manipulation. In this work, the grasped object is detected indirectly from current hand location and hand appearance. As illustrated in Figure 4, relative location (d_x, d_y) from the center of hand to the center of object is consistent to the hand orientation, and the object scale (W_o, H_o) is related to the size of hand opening. We formulate the hand and object detection as a two-stage problem. The first stage problem is hand segmentation which decides whether a pixel belongs to a hand, while the second stage problem is hand detection and object regression which detects real hand regions from hand segments and estimates object regions from hand regions.

For hand segmentation, we train a Fully Convolutional Network (FCN) which takes as input an image and outputs a hand probability map. FCN is a transformed architecture of existing CNNs to output spatial maps instead of classification scores and is commonly used in semantic segmentation. The training data contains a pair of image and annotated ground-truth hand mask. The loss function for hand segmentation network is the sum of per-pixel two-class (background and hand) softmax loss. Based on the obtained probability map, we can generate hand segments (blobs) by thresholding the probability map and get hand region proposals by drawing bounding boxes around the end of each hand blob. Hand region proposals are used as input of the second stage during model inference.

In the second stage, we train a Region-based Convolutional Neural Network (R-CNN) for hand and object detection (denoted as “DetectionNet”). The DetectionNet takes a hand region as input and has two sibling output layers. The first sibling layer outputs classification scores over three categories: “Background”, “LeftHand”, and “RightHand”. The reason why we set a category of “Background” for hand region proposals is to differentiate the skin-like non-hand background falsely segmented in the first stage. The second sibling layer outputs bounding-box regression offsets, $offset = (N_x, N_y, N_w, N_h)$, for the object grasped by the left hand and right hand respectively. The parameterization for $offset$ is given in the following equation set:

$$\begin{aligned}
 N_x &= \frac{d_x}{W_h}, N_y = \frac{d_y}{H_h} \\
 N_w &= \frac{W_o}{W_h}, N_h = \frac{H_o}{H_h}
 \end{aligned} \tag{8}$$

in which N_x and N_y specify scale-invariant transition from the center of hand to the center of object. N_w and N_h specify the scale ratio of object width and height with respect to the hand region.

Each training sample of DetectionNet is an image region labeled by a ground-truth hand label and a ground-truth bounding-box regression offset of the target object. We use a multi-task loss as in Girshick (2015). At testing, the output of classification layer is used as $\phi_h(P_h^s, I)$ in equation (5). The predicted offsets are used to calculate the standard object location as denoted by $P_{h \rightarrow o}^s$ in equation (4).

4.3 Training classifiers

To this extent, we have trained a hand segmentation network and a detection network to localize the hands and the manipulated objects. We now move forward to introduce the procedure of training appearance-based classifiers to provide visual evidence for grasp types, object attributes and actions.

With the cropped images of hands, we train grasp CNN (denoted as ‘‘GraspNet’’) to recognize the grasp types. The network takes pairs of cropped hand regions and ground-truth grasp type labels as training data, and output a vector of classification scores for different grasp types. The output is used as $\phi_g(P_h^s)$ in equation (5). Similar to GraspNet, we train object CNN (denoted as ‘‘ObjectNet’’) to recognize object attributes with the cropped images of objects. For training ObjectNet, pairs of cropped object regions and ground-truth object attribute labels are used as training data. The output is a vector of classification scores for different object attributes used as $\phi_o(P_o^s)$ in equation (6).

Unlike GraspNet and ObjectNet which use straightforward appearance cues from hand and object regions, the cues for training action classifier are more complex, involving both appearance and motion features. In this work, we train action CNN (denoted as ‘‘ActionNet’’) to recognize manipulation actions with two kinds of input. When action classification is conducted on single image, the whole image is used as input. When action classification is conducted on consecutive image sequence, optical flow images are used as input. The output of ActionNet is a vector of classification scores for different action classes used as $\phi_a(I)$ in equation (7).

4.4 Learning model parameters

Besides detectors and classifiers which are trained separately, model parameters are jointly learned from training data which weight different components of the model. At the parameter learning stage, annotations of hand and object bounding boxes, labels of grasp types, object attributes, and actions are used. We apply the DetectionNet and GraspNet to annotated hand bounding boxes to get hand detection scores and classification scores for the annotated grasp types. We apply the regression part of DetectionNet to hand bounding boxes together with the annotated object bounding boxes to get object detection scores, and apply ObjectNet to object bounding boxes to get classification scores for the annotated object attributes. We apply ActionNet to the whole image to get classification scores for the annotated action class. Then, we use a maximum likelihood approach to estimate the optimal model parameters $\{\alpha, \beta, \gamma, \zeta, \eta, \lambda, \xi\}$ with which

the model potential (1) achieves highest score on the training data.

4.5 Implementation details

Here we give the details of network architecture and training for CNNs. Since a better architecture of CNN is out of the scope of this work, we choose the networks that are commonly used with the consideration of practical performance in different tasks.

We use SegNet (Badrinarayanan et al. (2017)) as the architecture for FCN-based hand segmentation. SegNet is an encoder-decoder architecture for semantic segmentation and we adopt it for its good balance on accuracy and efficiency. The network has input size of $K \times 3 \times 360 \times 480$ and output size of $K \times 2 \times 360 \times 480$ where K is the batch size. We use a batch size of 8 and a fixed learning rate of $\gamma = 0.1$ for training the network.

We use CaffeNet (essentially AlexNet from Krizhevsky et al. (2012)) as the architecture for hand/object detection. CaffeNet is a small-size network which contains five convolutional layers and three fully-connected layers. We choose this network due to the limited size of annotated hand and object bounding boxes. The same network is used for grasp type classification and object attribute classification. The network has input size of $K \times 3 \times 227 \times 227$. For hand/object detection, the output layer is replaced with two sibling layers as described earlier (Section 4.2). For grasp type classification and object attribute classification, the output layer is replaced with a fully-connected layer and softmax over the number of categories. Due to the limited size of training samples, we adopt the finetuning approach and initialize CaffeNet using a pre-trained model from a large-scale dataset (ImageNet Deng et al. (2009)). We use a batch size of 100 and a fixed learning rate of $\gamma = 1e - 4$ for finetuning.

We use VGG-16 (Simonyan and Zisserman (2014)) as the network architecture for action classification. VGG-16 is a deep CNN model composed by 16 weight layers and has become popular due to its high performance achieved on ImageNet classification task. The network has input size of $K \times C \times 224 \times 224$, where K is the batch size and C is the number of channels. We set $C = 3$ for the input of a raw image, and $C = 20$ for the input of optical flow images. We finetune VGG-16 using pre-trained models from ImageNet and UCF101 (Soomro et al. (2012)) for input of raw image and optical flow images respectively. We use a batch size of 25 and a fixed learning rate of $\gamma = 5e - 4$ for finetuning.

5 Inference

Given a new image, we obtain the results for hand and object detection, as well as the classification of grasp types, object attributes and actions by inference on equation (1). We first initialize the model to get candidate hand and object locations and initial classification results (Section 5.1). Then we utilize an iterative method to update the inference results (Section 5.2).

5.1 Model initialization

To initialize the model inference, we first use the trained segmentation network to get a set of candidate hand

bounding boxes for each hand blob. Then we use the trained detection network to identify the hand side and remove falsely segmented background. Using the same network, we also get a set of candidate object bounding boxes for each valid hand bounding box. Finally, we initialize the classification results by applying the trained classifiers to the candidate hand and object bounding boxes and the current image respectively. Details of model initialization are given in the following steps.

Initializing hand locations. Hand blobs are first generated by thresholding the hand probability map obtained with the trained SegNet. Blobs beyond a certain range of area proportion are considered as false positive segments and discarded. Ellipse parameters (length of long/short axis, angle) are fitted to each hand blob and the forearm part is approximately removed by shortening the length of long axis to 1.5 times of the length of short axis. The remaining region of each blob is cropped with a bounding box as a reference hand bounding box $(X_{ref}, Y_{ref}, W_{ref}, H_{ref})$. For each reference hand bounding box, we further generate a set of candidate hand bounding boxes by sliding the reference bounding box in horizontal and vertical direction with a step of $\{-W_{ref}/8, 0, W_{ref}/8\}$ and $\{-H_{ref}/8, 0, H_{ref}/8\}$ respectively and also with a scale of $\{0.75, 1.0, 1.25\}$ for the width and height of each sliding window. We apply the trained R-CNN to all candidate hand bounding boxes to identify the hand side and remove the ones whose detection scores are below 0.8.

Initializing object locations. For each remained hand bounding box, we first estimate the reference object bounding box via the regression part of DetectionNet. Then we generate a set of candidate object bounding boxes for each reference object bounding box following the same routine as in generating candidate hand bounding boxes.

Initializing classification. We apply GraspNet to compute grasp type classification scores for each hand bounding box, apply ObjectNet to compute object attribution classification scores for each object bounding box, and apply ActionNet to compute action classification scores for current image. The labels of grasp type and object attribute are initialized with the class that has the highest score on the reference hand and object bounding boxes respectively. The action label is initialized with the class that has the highest action classification score.

5.2 Iterative inference

After model initialization, we iteratively update the inference results by performing the following steps.

Updating hand detection and grasp type classification. Based on the current results of action and object attribute labels, we update hand locations and labels of grasp type. The score of assigning grasp type g_i to the hand bounding box P_h^l of the left-side hand given action label a_k , grasp type label g_j at the other side and object attribute label o_m, o_n at both sides is represented as:

$$f(i, P_h^l) = \alpha_{k,i,j,m,n} + \beta_{i,m} + \zeta_l^T \cdot \phi_h(P_h^l, I) + \eta_i^T \cdot \phi_g(P_h^l). \quad (9)$$

The hand location and grasp type label are updated by selecting $(i^*, P_h^{l*}) = \arg \max f(i, P_h^l)$. The same inference is conducted for the right-side hand.

Updating object detection and object attribute classification. We first obtain the reference object bounding box $P_{h \rightarrow o}^l$ and a set of candidate object bounding boxes with the current bounding box of the left-side hand. Then, based on the current action label a_k , the object attribute label o_n at the other side and the grasp type label g_i, g_j of two sides, we assign object attribute o_m to the object bounding box P_o^l by optimizing the following score function:

$$f(m, P_o^l) = \alpha_{k,i,j,m,n} + \beta_{i,m} + \gamma_l \cdot p(P_o^l | P_{h \rightarrow o}^l) + \lambda_j^T \cdot \phi_o(P_o^l). \quad (10)$$

The same inference is conducted for the right-side object.

Updating action classification. Based on the current classification results of grasp type and object attribute, we update the action label by optimizing $\Psi_{FC}(G, O, A) + \Psi_A(A, I)$ with the enumeration of all possible action classes.

6 Evaluation

In this section, we evaluate our method on two public datasets. Datasets are first introduced in Section 6.1. Visualization of the learned model is shown in Section 6.2. Performance of the three recognition tasks are presented in Section 6.3 (grasp type and object attribute) and Section 6.4 (action). Finally, generalizability study is given in Section 6.5.

6.1 Dataset

We mainly evaluate our approach on the public GTEA Dataset (Fathi et al. (2011)) recorded with a head-mounted wearable camera. This dataset consists of 7 different cooking activities performed by 4 different subjects. Action annotations are provided with each containing a verb (action) and a set of objects with the beginning and ending frame. There are 10 action categories and 525 instances (video segments) in the original labels. To train and test the proposed model, we further annotated 1583 images with the following information: bounding boxes and grasp type labels of hands, bounding boxes and object attribute labels of the grasped objects. In Table 2, we summarize the name, proportion of each class for grasp types, object attributes and actions. Experiments of the three recognition tasks are evaluated using leave-one-subject-out cross-validation.

We also conduct experiments on GTEA Gaze Dataset (Fathi et al. (2012)) to study the generalizability of our method. This dataset consists of 17 sequences of cooking activities performed by 14 different subjects, also recorded with a wearable camera. The action verb and object categories with beginning and ending frame are annotated. Main difference of the two datasets is that they are recorded on different environments with different wearable devices, thereby causing appearance variation on similar activities. With similar annotation criterion, we further annotated 732 images for the experiments. We adopt the train/test splits for training and testing following previous work.

Table 2. Annotations of grasp types, object attributes and actions in GTEA Dataset. Action labels are provided in the dataset. Grasp types and object attributes are newly annotated in this work.

Grasp type			Object attribute			Action		
label	description	ratio	label	description	ratio	label	description	ratio
g01	power wrap	24.0%	o01	rigid-prismatic	25.4%	a01	close	10.0%
g02	precision wrap	8.8%	o02	deformable-prismatic	6.5%	a02	fold	1.5%
g03	parallel extension	18.7%	o03	rigid-flat	8.4%	a03	open	23.9%
g04	platform	4.9%	o04	deformable-flat	20.9%	a04	pour	13.1%
g05	precision sphere	6.1%	o05	rigid-round	12.1%	a05	put	14.7%
g06	power sphere	5.8%	o06	deformable-round	1.5%	a06	scoop	13.1%
g07	index finger extension	7.5%	o07	rigid-prismatic-flat	16.0%	a07	shake	0.4%
g08	writing tripod	5.1%	o08	rigid-flat-small	4.4%	a08	spread	9.7%
g09	lateral pinch	4.8%	o09	deformable-flat-small	4.9%	a09	stir	3.9%
g10	thumb-4 finger	2.0%				a10	take	9.7%
g11	thumb-2 finger	5.5%						
g12	tip pinch	4.6%						
g13	inferior pincer	2.2%						

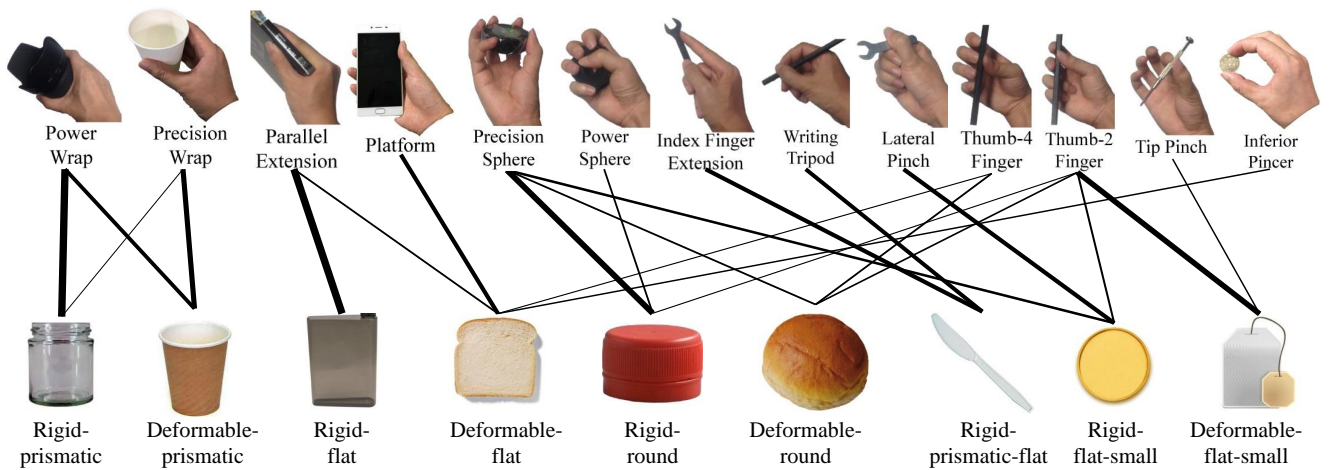


Figure 5. Visualization of the physical context learned on GTEA Dataset. The line strength indicates the strength of relationship between two classes.

6.2 Learned context

Based on visual evidence (Ψ_G, Ψ_O, Ψ_A in (1)) of 13 grasp types, 9 object attributes and 10 manipulation actions, our model learns contextual relationships ($\Psi_{FC}, \Psi_{PC}, \Psi_{SC}$ in (1)) between these components. In this section, we show the visualization of semantic context (Ψ_{FC} and Ψ_{PC}) learned from the GTEA Dataset.

Visualization of the learned physical context between grasp types and object attributes (Ψ_{PC}) is shown shown in Figure 5. The line strength in the figure demonstrates the strength of the context, which is estimated from β in (3). It can be seen that grasp types and attributes of the grasped objects are strongly correlated. For example, there is a strong connection between the *rigid-prismatic* object (such as a glass bottle) and the grasp type of *power wrap* which is the main hand pose affordable to hold the object stably in hand. Other strong connections can be found between the *rigid-flat* object and *parallel extension*, the *rigid-round* object and *precision sphere*, etc. The correlation between hands and objects helps us to better recognize grasp types and object attributes together. For example, it is more likely that the *rigid-round* object is

grasped by *precision sphere* than by *thumb-2 finger*. From Figure 5, we also observe dexterous hand-object interactions that the same object can be held by multiple grasp types and the same grasp type affords to manipulate more than one types of objects. Nevertheless, the dexterous aspect of hand-object interactions provides important information for understanding manipulation activities. For example, the connections between the *rigid-prismatic-flat* object and two different grasp types are related to two different actions: *scoop* and *spread* as occurred in the dataset.

Visualization of the learned functional context between actions, grasp types and object attributes (Ψ_{FC}) is shown in Figure 6. Specifically, we visualize the strength of action-hand and the action-object relationships separately, which are estimated by marginalizing α in (2) with respect to object attributes and grasp types respectively. Figure 6 demonstrates that our model learns meaningful hand-action-object interactions in manipulation activities. One important observation is that grasp type together with object attribute provide complementary information which is useful in characterizing different actions. Taking *deformable-flat-small* object (such as a tea pack) for example, it is

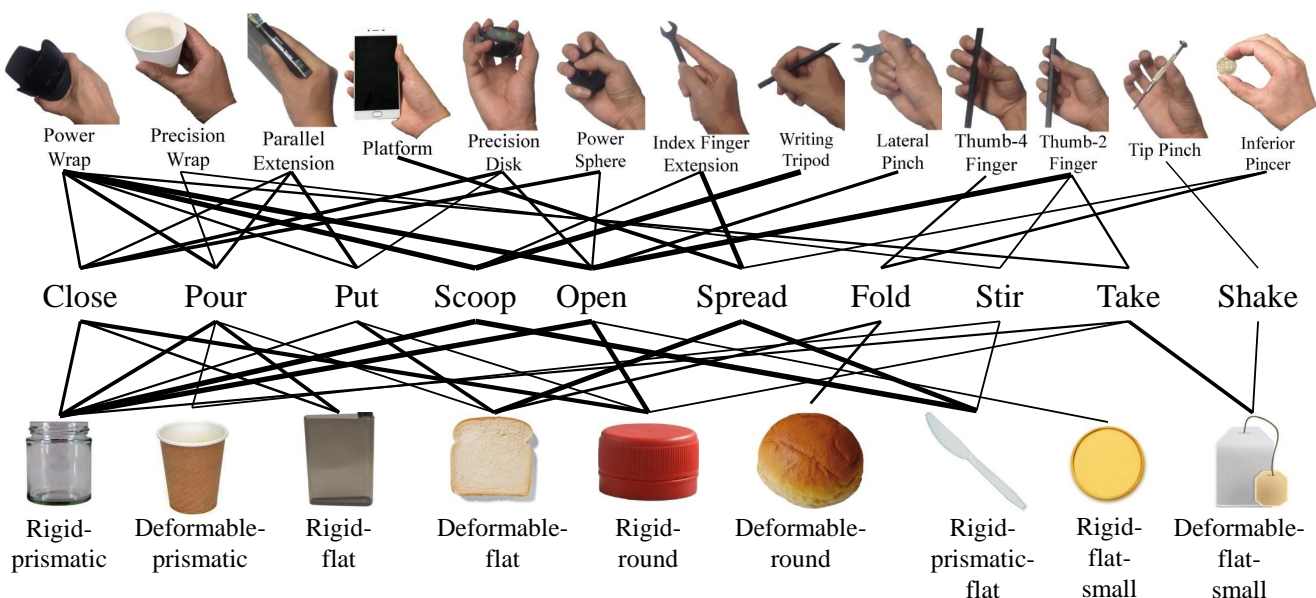


Figure 6. Visualization of the functional context learned on GTEA Dataset. The line strength indicates the strength of relationship between two classes.

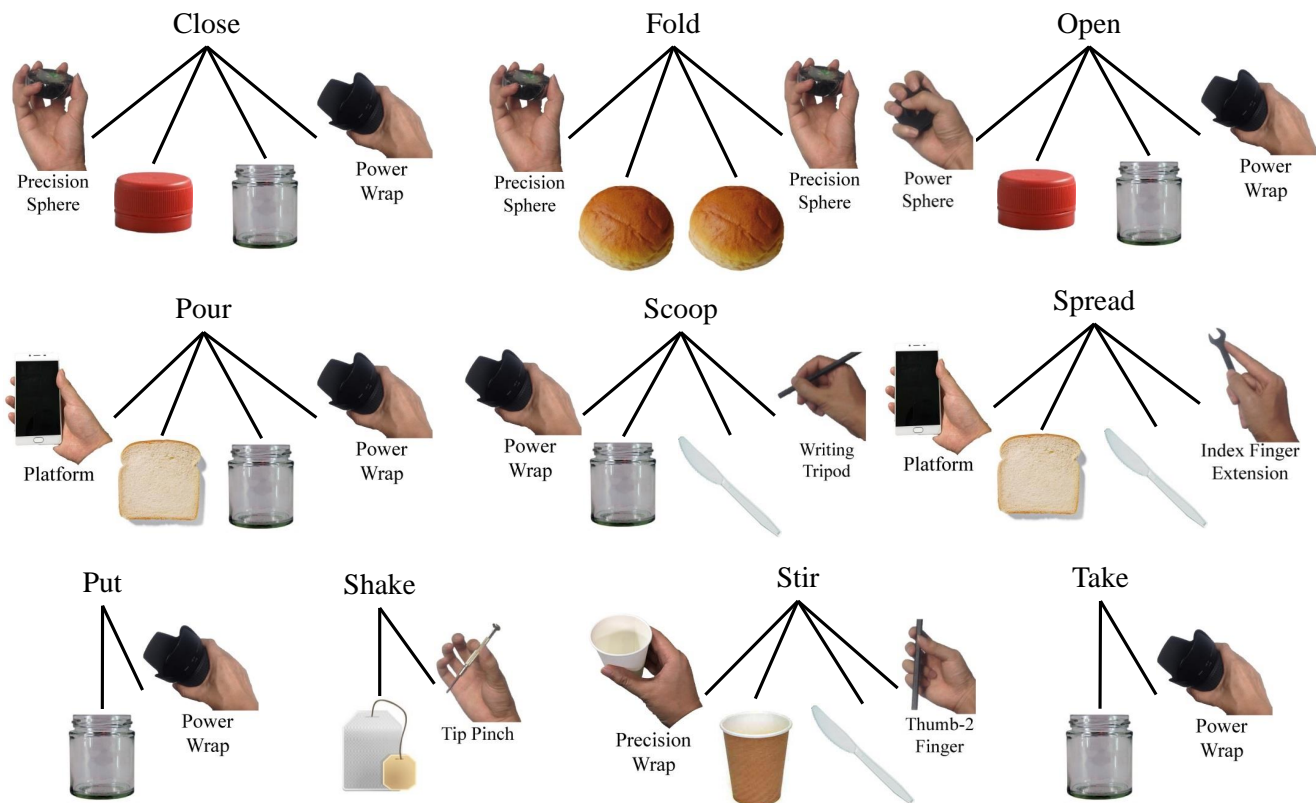


Figure 7. Visualization of the most probable combinations of grasp types and object attributes conditioned on each action class.

grasped with *thumb-2 finger* during the action of *take*, while grasped with *tip pinch* during the action of *shake*. Furthermore, we observe that some actions involve complex hand-object interactions and information from both hands are needed to distinguish between them. Taking *close* and *pour* for example, although both actions involve a hand holding a bottle-like object on one side, on the other side different objects (such as *rigid-round* bottle cap and *deformable-prismatic* cup) are held by different grasp types

(such as *precision sphere* and *precision wrap*) respectively. Nevertheless, these complex interactions are learned in our proposed functional context. Figure 7 illustrates the most likely combinations of grasp types and object attributes for each action class. It can be seen that 7 out of 10 action classes are most likely characterized by bimanual operation.

In the following sections, we will show how the learned context helps improve the recognition performance of grasp types, object attributes and actions.

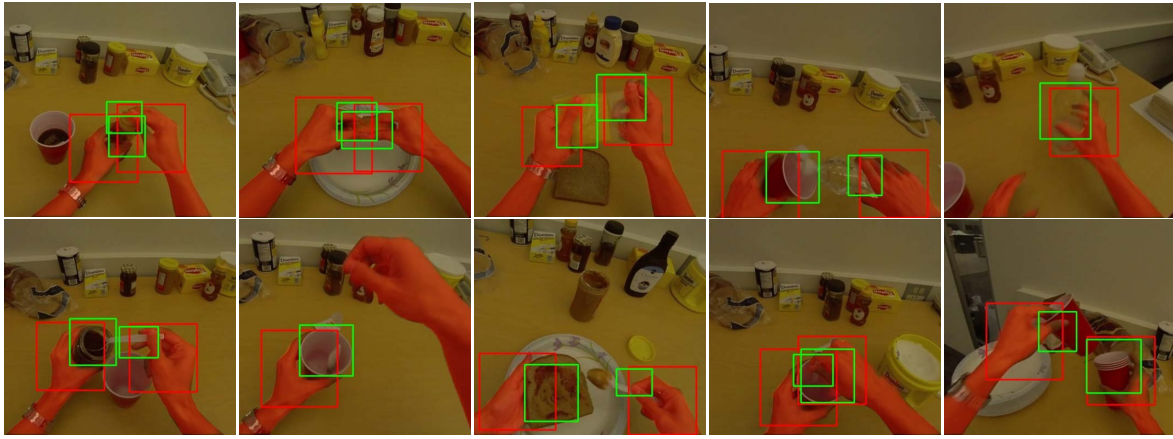


Figure 8. Hand and object detection on GTEA Dataset. Hand probability map (red) is overlapping with the raw image. Hand bounding box (red) and object bounding box (green) are drawn on top of the image. Examples are selected from 10 different actions (Top 5: close, fold, open, pour, put; Bottom 5: scoop, shape, spread, stir, take).

6.3 Recognition of grasp type and object attribute

Hand and object detection. As described in Section 4.2, hand and object detection is formulated as a two-stage problem. In the first stage, we train a hand segmentation network to generate hand probability map for each image which is then used for computing hand region proposals. We use raw images and hand masks provided with GTEA Dataset as training data for hand segmentation network. The input image dimension is down-sampled to the input size of the network and the output probability map is up-sampled to the original size. Hand region proposals are generated by thresholding the probability map and drawing bounding boxes around the ends of each hand blob. In the second stage, we train a detection network to filter candidate hand bounding boxes and regress the bounding box offsets for the grasped objects. The generated candidate hand and object bounding boxes are used as input of the model inference and the final hand/object locations are estimated with corresponding grasp types/object attributes.

Qualitative results of hand and object detection in different actions are shown in Figure 8. The detected hand and object bounding boxes match well with the real hand and object locations, even though the background is cluttered and the grasped objects are partially occluded. The results demonstrate the effectiveness of hand segmentation network and the feasibility of detecting the grasped objects simply from hand appearance.

Grasp type recognition. Here we evaluate the recognition performance of 13 grasp types on GTEA Dataset. We use GraspNet as the baseline in which the grasp type is assigned to the category with which highest score obtains in the output softmax layer. Note that the GraspNet is also used for initializing the grasp classification scores in equation (5) of our model. We also compare our method with another baseline (denoted as “GraspNet+object context”) in which the attribute information from the grasped object serves as object context to improve the recognition performance. This method was first used in the work of Cai et al. (2016).

Table 3 shows grasp type recognition results of different methods. It can be observed that our method achieves the

best performance. Compared with other baselines without or with limited context, our method explores the semantic relationship with the grasped object and the performed action, which helps to differentiate grasp types that are visually ambiguous. Taking *g04 (platform)* for example, the GraspNet achieves accuracy of 75.0%, including context from object improves the performance to 78.2%, and our method further enhances the performance to 87.8%. Two reasons might explain the performance improvement. On the one hand, object attributes provide physical constraints on a small set of grasp types which are affordable to hold the object. On the other hand, our method also takes functional constraints by recognizing different manipulation actions (e.g., recognition of *spread*), which further helps to differentiate visually similar grasp types.

Table 3. Grasp type recognition results on GTEA Dataset. Classification accuracy is used as evaluation metric.

Method	GraspNet	GraspNet+ object context	Our method
g01	65.5%	63.2%	68.3%
g02	72.1%	74.5%	74.5%
g03	63.8%	71.4%	72.2%
g04	75.0%	78.2%	87.8%
g05	37.1%	46.5%	48.0%
g06	40.0%	42.8%	46.1%
g07	53.4%	54.5%	57.1%
g08	68.8%	72.4%	73.6%
g09	23.5%	23.5%	27.5%
g10	44.4%	52.9%	50.0%
g11	34.7%	35.2%	37.5%
g12	37.5%	37.5%	48.0%
g13	21.0%	26.6%	21.0%
Overall	51.4%	55.5%	57.5%

Object attribute recognition. Similar to grasp type recognition, we compare our method with two baselines without (“ObjectNet”) or with limited context (“ObjectNet+grasp context”), and show how object attribute recognition is improved by contextual information from the grasp

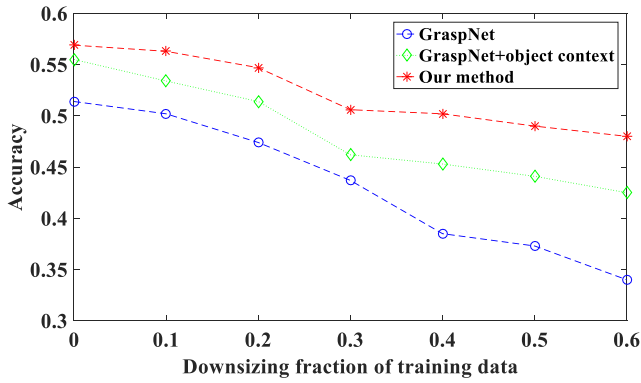


Figure 9. Performance variation of grasp type recognition at different sizes of training data. The horizontal axis shows the fraction of training data that are removed. Downsizing fraction of 0.1 means 10% of training data are removed.

types and actions. As shown in Table 4, overall accuracy for 9 different object attributes is 58.9% from ObjectNet. Grasp context improves the accuracy by 2.9%, and our method further improves the performance by 2.1%. It is interesting to see that the performance improvement for o03 (9.1%) is consistent with the that for g03 (8.4%). Actually, g03 (*parallel extension*) and o03 (*rigid flat*) are strongly correlated in HOM activities and the mutual context learned between the two helps to enhance the recognition performance in both tasks.

Table 4. Object attribute recognition results on GTEA Dataset. Classification accuracy is used as evaluation metric.

Method	ObjectNet	ObjectNet+grasp context	Our method
o01	65.7%	64.4%	69.2%
o02	83.6%	85.1%	87.2%
o03	70.9%	78.6%	80.0%
o04	78.4%	85.1%	88.8%
o05	43.8%	41.6%	45.9%
o06	37.5%	42.8%	42.8%
o07	63.9%	68.2%	69.0%
o08	25.0%	30.7%	28.5%
o09	14.8%	14.8%	22.2%
Overall	58.9%	61.8%	63.9%

Robustness study. We have shown in Table 3 and Table 4 that the recognition performance of both grasp types and object attributes have been improved by our method. To get a better understanding about the effectiveness of context, we further evaluate the recognition performance in difficult situations where annotated labels are insufficient to train reliable classifiers. Specifically, we gradually downsize the training data of grasp types and object attributes respectively and evaluate the performance of different methods. Figure 9 demonstrates the performance variation of grasp type recognition. As we increase the downsizing fraction, performance of all methods decreases. However, the methods using context (GraspNet+object context, and our method) degrade much less slowly than CNN-based method (GraspNet), and the performance gap between

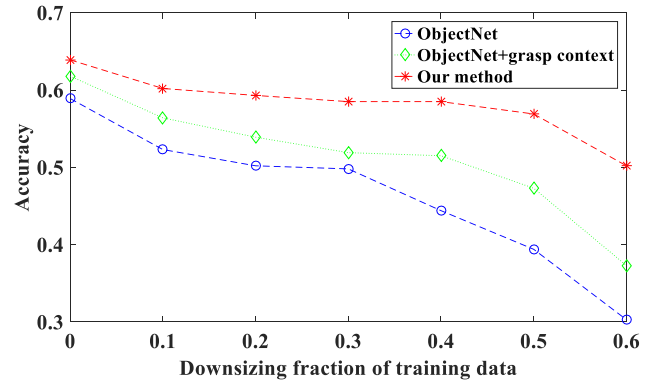


Figure 10. Performance variation of object attribute recognition at different sizes of training data.

GraspNet and our method increases nearly to 15% when 60% of training data are removed. Similar performance variation for object attribute recognition can be observed in Figure 10. The results demonstrate the importance of contextual relationships in multi-task recognition when sufficient annotations are not available for all tasks.

6.4 Action recognition

In this section, we evaluate the action recognition performance of three different methods. The first method uses action CNN (ActionNet) to recognize actions directly from visual observation, often in terms of image appearance or optical flow-based motion. In Ma et al. (2016), a two-stream CNN model incorporating information from both appearance and motion has achieved state-of-the-art performance in egocentric action recognition. Note that a better CNN architecture is not the focus of this work, and we are more interested in how contextual relationships could improve action recognition performance of different CNN models. Therefore, we train ActionNet based on single image and optical flow images separately (denoted as “ActionNet-rgb” and “ActionNet-flow” respectively). The second method models manipulation action only by its functional components of hands and objects, more specifically, of hand grasp types and object attributes. Instead of visual observation as used in the first method, only contextual information from grasp types and object attributes are used in the second method (denoted as “Context only”). Finally, in our method, both visual observation and contextual information are utilized in the proposed model. We denote our methods as “Ours-rgb” and “Ours-flow”, in which ActionNet-rgb and ActionNet-flow are used to provide visual evidence for actions respectively.

Table 5 shows action recognition results on different action classes and the overall accuracy. ActionNet-rgb is used as baseline to show how performance could be improved for image-based recognition. Our method achieves best performance and outperforms ActionNet-rgb by over 10%, demonstrating the effectiveness of our model in image-based action recognition. It is also important to note that the second method with only contextual information outperforms ActionNet-rgb by 6.9%. Since the contextual information comes from visual recognition of hand and object regions, the result actually indicates that it is more

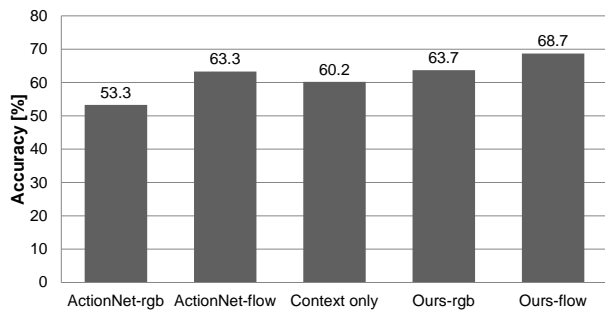


Figure 11. Action classification results of different methods on the GTEA dataset. Classification accuracy is used to evaluate the performance.

efficient to model actions from appearance of interaction than from the whole image.

Table 5. Image-based action recognition results on GTEA Dataset. Classification accuracy is used as evaluation metric.

Method	ActionNet-rgb	Context only	Ours-rgb
a01	29.0%	28.0%	37.7%
a02	40.0%	100.0%	66.6%
a03	56.6%	55.2%	64.3%
a04	46.6%	78.6%	71.8%
a05	67.9%	61.1%	69.2%
a06	31.1%	76.7%	56.0%
a07	23.9%	28.2%	29.0%
a08	82.3%	64.2%	88.4%
a09	42.8%	58.3%	50.0%
a10	55.1%	51.0%	62.7%
Overall	53.3%	60.2%	63.7%

Figure 11 summarizes the overall performance of different methods. ActionNet-flow outperforms ActionNet-rgb by 10%, showing that motion information from multiple consecutive images has obvious advantage of discriminative power over appearance information from a single image. However, the performance of “Ours-rgb” is even slightly better than ActionNet-flow, indicating the ability of context to boost the image-based action recognition to the extent that can only be achieved from video. The best performance of 68.7% accuracy is achieved from “Ours-flow”, outperforming ActionNet-flow by 5.4%.

6.5 Generalizability study

By far we have shown that our method with the learned contextual relationships has achieved significant performance improvement on GTEA Dataset. However, generalizability is always an issue that how the research findings and conclusions from a study on a sample population could generalize to a larger population. In this section, we study the generalizability of our method by evaluating its performance across two different datasets (GTEA Dataset and GTEA Gaze Dataset).

We first evaluate the cross-dataset performance of CNN-based classifiers. Although CNNs are not the main novelty of our method, it is important to know their generability across different datasets, as they are widely used in various

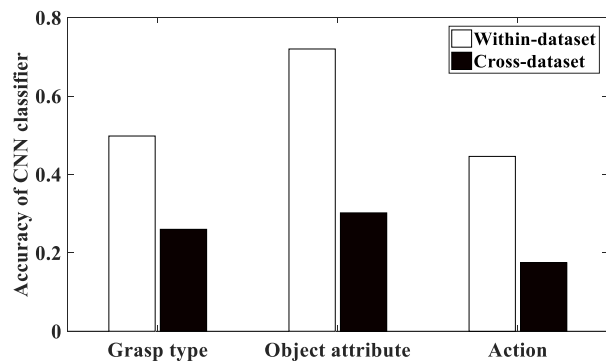


Figure 12. Generalizability evaluation of CNN-based classifiers by classification accuracy of grasp types, object attributes and actions. For “within-dataset”, CNN classifiers are trained (or finetuned) and tested on the training/testing division of GTEA Gaze Dataset. For “cross-dataset”, CNN classifiers are trained on GTEA Dataset and tested on GTEA Gaze Dataset.

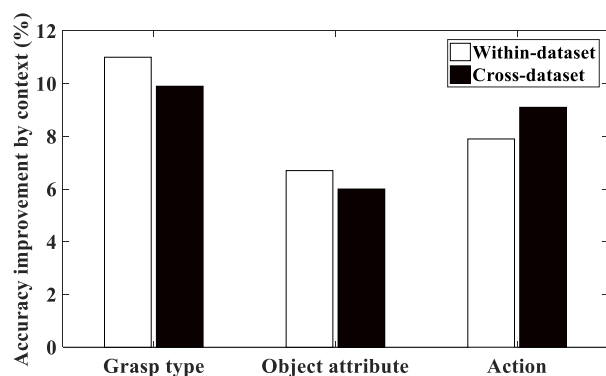


Figure 13. Generalizability evaluation of contextual relationship by classification accuracy improvement of grasp types, object attributes and actions. Experiments are conducted on GTEA Gaze Dataset with CNN classifiers trained on the same dataset. For “within-dataset”, context learned on GTEA Gaze Dataset is used, while for “cross-dataset”, context learned on GTEA Dataset is used.

recognition problems and also provide visual evidence in our method. Figure 12 shows cross-dataset performance of CNN classifiers by classification accuracy of grasp types, object attributes and actions respectively. Large performance drop could be seen for all three classification tasks. The results indicate that CNN classifiers are sensitive to appearance variation (kind of overfitting to the training data), and can not be directly applied to other datasets without sufficiently large training data or finetuning on the target data space.

We then evaluate the cross-dataset performance of the contextual relationships studied in this work. Specifically, we are interested in how the context learned from one dataset (GTEA Dataset) could improve the recognition performance in another dataset (GTEA Gaze Dataset). Figure 13 shows cross-dataset performance of context by the improvement of classification accuracy of grasp types, object attributes and actions respectively. Compared with the context learned on the current GTEA Gaze Dataset, the context learned on previous GTEA Dataset achieves comparative accuracy improvement (and even larger improvement for action classification), indicating good generalizability of contextual relationships to different datasets of HOM activities. More

importantly, the generalizability study shows the importance of exploring common knowledge shared within the same problem domain in the realization of a more general vision recognition system.

7 Conclusion and future work

In this work, we propose a novel method for understanding hand-object manipulation, in which grasp types, object attributes and actions are recognized in an unified framework. Considering various contextual relationships between actions, hands and objects, we construct a context model to optimize the three tasks together.

Experiments on public egocentric activity datasets illustrate that the proposed method achieves best recognition performance for all three tasks, verifying the effectiveness of jointly modeling grasp types, object attributes and action. The visualization and analysis of the learned context support our hypothesis that the contextual relationships between action, hand and object play an important role in understanding hand-object manipulation.

In current work, the contextual relationships between actions, hands and objects are studied in a static model, in which the relationships remain unchanged during a manipulation action. However, in certain action such as opening a tight bottle cap, hand grasp type changes from the beginning (*power sphere*) to the end (*precision sphere*). One direction of our future work is to study the contextual relationships dynamically in order to capture the temporal evolution of hand-object interaction patterns in different manipulation actions. Besides, to train our model, we need to annotate lots of information in each training image, which limits the scale of data we can explore. Therefore, another direction of our future work is to develop an efficient approach (such as unsupervised learning) for understanding hand-object manipulation from a large amount of data.

References

- Badrinarayanan V, Kendall A and Cipolla R (2017) Segnet: A deep convolutional encoder-decoder architecture for image segmentation. *IEEE Transactions on Pattern Analysis and Machine Intelligence*.
- Bullock I, Feix T and Dollar A (2013a) Finding small, versatile sets of human grasps to span common objects. In: *IEEE International Conference on Robotics and Automation (ICRA)*. IEEE, pp. 1068–1075.
- Bullock I, Zheng J, Rosa S, Guertler C and Dollar A (2013b) Grasp frequency and usage in daily household and machine shop tasks. *IEEE Transactions on Haptics* 6(3): 296–308.
- Cai M, Kitani K and Sato Y (2015) A scalable approach for understanding the visual structures of hand grasps. In: *2015 IEEE International Conference on Robotics and Automation (ICRA)*. IEEE, pp. 1360–1366.
- Cai M, Kitani K and Sato Y (2016) Understanding hand-object manipulation with grasp types and object attributes. In: *Robotics: Science and Systems Conference (RSS)*. pp. 1–10.
- Cai M, Kitani K and Sato Y (2017) An ego-vision system for hand grasp analysis. *IEEE Transactions on Human-Machine Systems* 47(4): 524–535.
- Cutkosky M (1989) On grasp choice, grasp models, and the design of hands for manufacturing tasks. *IEEE Transactions on Robotics and Automation* 5(3): 269–279.
- Deng J, Dong W, Socher R, jia Li L, Li K and Fei-fei L (2009) Imagenet: A large-scale hierarchical image database. In: *IEEE Conference on Computer Vision and Pattern Recognition (CVPR)*. pp. 248–255.
- Dollar A (2014) Classifying human hand use and the activities of daily living. In: *The Human Hand as an Inspiration for Robot Hand Development*. Springer, pp. 201–216.
- Farhadi A, Endres I, Hoiem D and Forsyth D (2009) Describing objects by their attributes. In: *IEEE Conference on Computer Vision and Pattern Recognition (CVPR)*. IEEE, pp. 1778–1785.
- Fathi A, Farhadi A and Rehg J (2011) Understanding egocentric activities. In: *IEEE International Conference on Computer Vision (ICCV)*. IEEE, pp. 407–414.
- Fathi A, Li Y and Rehg J (2012) Learning to recognize daily actions using gaze. In: *European Conference on Computer Vision (ECCV)*. Springer, pp. 314–327.
- Feix T, Bullock I and Dollar A (2014a) Analysis of human grasping behavior: Object characteristics and grasp type. *IEEE Transactions on Haptics* 7(3): 311–323.
- Feix T, Bullock IM and Dollar AM (2014b) Analysis of human grasping behavior: Correlating tasks, objects and grasps. *IEEE transactions on haptics* 7(4): 430–441.
- Feix T, Pawlik R, Schmiedmayer H, Romero J and Kragic D (2009) A comprehensive grasp taxonomy. In: *Robotics: Science and Systems Workshop on Understanding the Human Hand for Advancing Robotic Manipulation*. pp. 2–3.
- Feix T, Romero J, Schmiedmayer H, Dollar A and Kragic D (2016) The grasp taxonomy of human grasp types. *IEEE Transactions on Human-Machine Systems* 46(1): 66–77.
- Gilster R, Hesse C and Deubel H (2012) Contact points during multidigit grasping of geometric objects. *Experimental Brain Research* 217(1): 137–151.
- Girshick R (2015) Fast R-CNN. In: *Proceedings of the International Conference on Computer Vision (ICCV)*. pp. 1440–1448.
- Hamer H, Schindler K, Koller-Meier E and Van Gool L (2009) Tracking a hand manipulating an object. In: *Computer Vision, 2009 IEEE 12th International Conference On*. IEEE, pp. 1475–1482.
- Huang D, Ma M, Ma W and Kitani K (2015) How do we use our hands? discovering a diverse set of common grasps. In: *Proceedings of the IEEE Conference on Computer Vision and Pattern Recognition (CVPR)*. pp. 666–675.
- Kang S and Ikeuchi K (1993) Toward automatic robot instruction from perception-recognizing a grasp from observation. *IEEE Transactions on Robotics and Automation* 9(4): 432–443.
- Kjellstrom H, Romero J and Kragic D (2008) Visual recognition of grasps for human-to-robot mapping. In: *IEEE/RSJ International Conference on Intelligent Robots and Systems (IROS)*. IEEE, pp. 3192–3199.
- Klatzky RL, McCloskey B, Doherty S, Pellegrino J and Smith T (1987) Knowledge about hand shaping and knowledge about objects. *Journal of Motor Behavior* 19(2): 187–213.
- Krizhevsky A, Sutskever I and Hinton G (2012) Imagenet classification with deep convolutional neural networks. In: *Advances in neural information processing systems (NIPS)*. pp.

- 1097–1105.
- Kumar N, Berg A, Belhumeur P and Nayar S (2009) Attribute and simile classifiers for face verification. In: *IEEE 12th International Conference on Computer Vision (ICCV)*. IEEE, pp. 365–372.
- Lampert C, Nickisch H and Harmeling S (2009) Learning to detect unseen object classes by between-class attribute transfer. In: *IEEE Conference on Computer Vision and Pattern Recognition (CVPR)*. IEEE, pp. 951–958.
- Li Y, Ye Z and Rehg J (2015) Delving into egocentric actions. In: *The IEEE Conference on Computer Vision and Pattern Recognition (CVPR)*. pp. 287–295.
- Liu J, Nakamura Y and N P (2014) A taxonomy of everyday grasps in action. In: *IEEE International Conference on Humanoid Robots (Humanoids)*. IEEE, pp. 3570–3577.
- Ma M, Fan H and Kitani K (2016) Going deeper into first-person activity recognition. In: *The IEEE Conference on Computer Vision and Pattern Recognition (CVPR)*. pp. 1894–1903.
- Napier J (1956) The prehensile movements of the human hand. *Journal of bone and Joint surgery* 38(4): 902–913.
- Oikonomidis I, Kyriazis N and Argyros A (2011) Full dof tracking of a hand interacting with an object by modeling occlusions and physical constraints. In: *IEEE International Conference on Computer Vision (ICCV)*. IEEE, pp. 2088–2095.
- Parikh D and Grauman K (2011) Relative attributes. In: *IEEE International Conference on Computer Vision (ICCV)*. IEEE, pp. 503–510.
- Pirsiavash H and Ramanan D (2012) Detecting activities of daily living in first-person camera views. In: *IEEE Conference on Computer Vision and Pattern Recognition (CVPR)*. IEEE, pp. 2847–2854.
- Rogez G, Supancic JS III and Ramanan D (2015) Understanding everyday hands in action from rgb-d images. In: *The IEEE International Conference on Computer Vision (ICCV)*. IEEE, pp. 4325–4333.
- Romero J, Kjellström H, Ek C and Kragic D (2013) Non-parametric hand pose estimation with object context. *Image and Vision Computing* 31(8): 555–564.
- Sadeghi M and Farhadi A (2011) Recognition using visual phrases. In: *IEEE Conference on Computer Vision and Pattern Recognition (CVPR)*. IEEE, pp. 1745–1752.
- Santello M, Flanders M and Soechting J (1998) Postural hand synergies for tool use. *The Journal of Neuroscience* 18(23): 10105–10115.
- Saran A, Teney D and Kitani K (2015) Hand parsing for fine-grained recognition of human grasps in monocular images. In: *IEEE/RSJ International Conference on Intelligent Robots and Systems (IROS)*. IEEE, pp. 5052–5058.
- Siddiquie B, Feris R and Davis L (2011) Image ranking and retrieval based on multi-attribute queries. In: *IEEE Conference on Computer Vision and Pattern Recognition (CVPR)*. IEEE, pp. 801–808.
- Simonyan K and Zisserman A (2014) Very deep convolutional networks for large-scale image recognition. *CoRR* abs/1409.1556.
- Singh V, Khan F and Nevatia R (2010) Multiple pose context trees for estimating human pose in object context. In: *IEEE Conference on Computer Vision and Pattern Recognition-Workshop*. IEEE, pp. 17–24.
- Soomro K, Zamir AR and Shah M (2012) Ucf101: A dataset of 101 human actions classes from videos in the wild. *arXiv preprint arXiv:1212.0402*.
- Vedaldi A, Mahendran S, Tsogkas S, Maji S, Girshick R, Kannala J, Rahtu E, Kokkinos I, Blaschko M and Weiss D (2014) Understanding objects in detail with fine-grained attributes. In: *IEEE Conference on Computer Vision and Pattern Recognition (CVPR)*. IEEE, pp. 3622–3629.
- Yang Y, Li Y, Fermuller C and Aloimonos Y (2015a) Grasp type revisited: A modern perspective of a classical feature for vision. In: *IEEE Conference on Computer Vision and Pattern Recognition*. IEEE, pp. 400–408.
- Yang Y, Li Y, Fermuller C and Aloimonos Y (2015b) Robot learning manipulation action plans by” watching” unconstrained videos from the world wide web. In: *Twenty-Ninth AAAI Conference on Artificial Intelligence*. pp. 3686–3692.
- Yao B and Fei-Fei L (2010) Modeling mutual context of object and human pose in human-object interaction activities. In: *IEEE Conference on Computer Vision and Pattern Recognition (CVPR)*. IEEE, pp. 17–24.
- Zhang N, Paluri M, Ranzato M, Darrell T and Bourdev L (2014) Panda: Pose aligned networks for deep attribute modeling. In: *IEEE Conference on Computer Vision and Pattern Recognition (CVPR)*. IEEE, pp. 1637–1644.
- Zheng J, De La Rosa S and Dollar A (2011) An investigation of grasp type and frequency in daily household and machine shop tasks. In: *IEEE International Conference on Robotics and Automation (ICRA)*. IEEE, pp. 4169–4175.